Manipulation of linearly polarized states in a diode-pumped YAG/Tm:YAG/YAG bulk laser

Yanying Li,[1,3,†] Weidong Chen,[1,†] Haifeng Lin,[1,3] Da Ke,[1] Ge Zhang,[1,4] and Yung-Fu Chen[2,5]

[1]*Key Laboratory of Optoelectronic Materials Chemistry and Physics, Fujian Institute of Research on the Structure of Matter, Chinese Academy of Sciences, Fuzhou, Fujian 350002, China*

[2]*Department of Electrophysics, National Chiao Tung University, Hsinchu 30010, Taiwan*

[3]*University of Chinese Academy of Sciences, Beijing 100049, China*

[4]*e-mail: zhg@fjirsm.ac.cn*

[5]*e-mail: yfchen@cc.nctu.edu.tw*

Received January 23, 2014; revised February 18, 2014; accepted February 19, 2014; posted February 20, 2014 (Doc. ID 204636); published March 24, 2014

We experimentally demonstrated the manipulation of 2 μm linearly polarized states in a diode-pumped YAG/Tm:YAG/YAG laser with high polarization extinction ratio of 28 dB for the very first time to the best of our knowledge. A stable linearly polarized state of 2 μm was achieved without using any specific intracavity optical polarization-selected elements. The unexpected phenomenon of tunable linear polarization directions was observed. Multidistinct linear polarization directions were experimentally obtained, including the peculiar case of switchable orthogonally linear polarization directions. © 2014 Optical Society of America

OCIS codes: (140.3480) Lasers, diode-pumped; (140.3580) Lasers, solid-state; (260.5430) Polarization.
http://dx.doi.org/10.1364/OL.39.001945

The polarization properties of 2 μm lasers are vital components for various applications, such as nonlinear frequency conversion [1], polarized laser beam combining [2], acousto-optical modulation [3], and interferometers [4]. Tm^{3+}-doped yttrium aluminum garnet ($Tm:Y_3Al_5O_{12}$, Tm:YAG) crystal exhibits broad absorption and stimulated spectra [5]. Its two-for-one cross-relaxation process enables high efficient laser operation [6], and its attractive thermo-mechanical properties [7] also allow high-power operation with reduced probability of fracture. Therefore Tm:YAG has been identified to be an excellent candidate for obtaining high-power operation near the 2 μm spectral region. As the host crystal, in particular, YAG has a cubic symmetry characteristic, thus making it optically isotropic. An unpolarized laser oscillation is expected in a free-running Tm:YAG laser. Conventionally, realization of polarization emission in the YAG host laser is conducted by using some optical components such as intracavity Brewster plates [8], thin-film polarizers, or linearly polarized pump light [9].

Alternatively, some special approaches were used to obtain spontaneous linear polarization emission, especially the recently reported polarization manipulated solid-state laser being achieved with six crystalline orientations in Yb:YAG microchip laser [10,11]. Moreover, linearly polarized laser output was observed in Cr,Nd:YAG passively switched lasers [12] and also had been demonstrated in Yb:YAG/Cr^{4+}:YAG combination passively *Q*-switched microchip lasers [13]. But until now there have been no relevant reports on direct linear polarization emission around 2 μm in diode-pumped Tm:YAG laser without using any specific intracavity optical polarization-selected elements. In this Letter, we reported experimental manipulation of 2 μm linearly polarized states in diode-pumped YAG/Tm:YAG/YAG crystalline laser for the first time to the best of our knowledge. Without using any specific intracavity optical polarization-selected elements, the fairly stable linear polarized emission with maximum polarization extinction ratio (PER) of 28 dB was obtained. The optimal linearly polarized operation was achieved for the output coupler with transmission of 5%. The corresponding slope efficiency with respect to the absorbed pump power was up to 52.3%. Besides, tunable linear polarization directions with 11 distinct directions were experimentally achieved, including the switchable orthogonally linear polarization directions.

The laser configuration for the linearly polarized operation of 2 μm YAG/Tm:YAG/YAG crystalline laser was schematically shown in Fig. 1.

The pumping source was an 808 nm fiber-coupled (NA = 0.22, 200 μm core diameter) laser diode (Limo). In contrast to 785 nm pumping source, wing-pumping at 808 nm will reduce the quantum defect so as to partly release the thermal lensing effect while still yielding sufficient population inversion to overcome the ground-state reabsorption therefore realizing efficient laser operation [14]. The active element was a $\Phi 3 \times 25\ \mathrm{mm}^3$ dual-end diffusion-bonded composite YAG/Tm:YAG/YAG crystal. It was fabricated by directly bounding two 5 mm undoped segments to both facets of the 15 mm 3.5 at. % Tm:YAG crystal. Both sides of the crystal were antireflection coated at 780–810 nm and 1950–2100 nm.

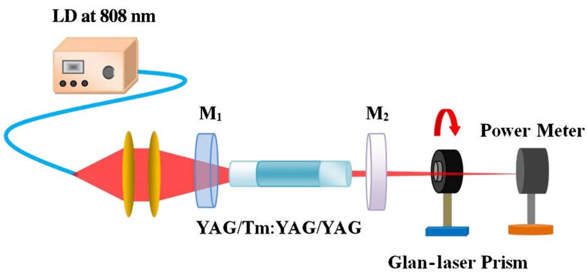

Fig. 1. Schematic diagram of the linearly polarized opeartion YAG/Tm:YAG/YAG crystalline laser.

0146-9592/14/071945-04$15.00/0 © 2014 Optical Society of America

The specific improvement of the composite crystal resulted in the reduction of peak temperature rise in active segment and alleviation of the thermal lensing effect [15,16]. The crystal was wrapped with indium foil and mounted on a copper heat sink with a thermo-electric cooler module to maintain a constant temperature around 286.5 K for efficient heat dissipation. The pump beam was collimated onto the laser crystal by a pair of plano-convex lenses with an imaging ratio of 1:2, which provided a pump spot radius of around 200 μm. The pump beam was delivered through the input mirror (M_1), with high transmission ($T > 96\%$) at the pump wavelength and high reflection at the wavelengths in the range of 2000–2100 nm ($R > 99.93\%$). The output coupler (M_2) was coated with partial transmission at the wavelengths in the 2010–2020 nm range. The overall resonator length was typically around 65 mm. The polarization states of output laser were analyzed by using a Glan-Laser prism (Ultra Photonics, Inc. made by Calcite with transmission of 350–2300 nm) in combination with a power meter.

Initially, the polarization property of a YAG/Tm:YAG/YAG bulk laser was investigated by using a plane–parallel resonator configuration with output coupling transmission ($T_{\rm OC}$) of 5%. The unpolarized pumping source at 808 nm was adopted for eliminating the influence of linearly polarized pumping source. Linearly polarized operation with high PER was achieved by carefully aligning the resonator with the help of monitoring the real-time output power after passing through the Glan-Laser prism. The linear polarization state was observed with the linear polarization direction located at the angle of 90° (we defined the horizontal as 0° and vertical as 90°). Figure 2 depicted the typical linear polarization operation of YAG/Tm:YAG/YAG bulk laser measured at the maximum absorbed pump power.

A stable linearly polarized lasing with high PER of 26 dB was obtained. An unexpected phenomenon was observed during the experiment, whereby the specific linear polarization directions of output laser were tunable only by realigning the resonator without rotating the crystalline-orientation. Figure 3 showed experimentally obtained tunable linear polarization directions. With the help of changing the angles of Glan-Laser prism, we realized four other distinct linear polarization directions as a function of polarizer angle, at 0°, 120°, 150°, and 170°, respectively. They were all achieved under the

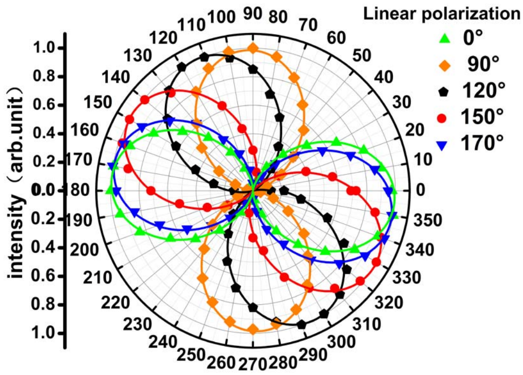

Fig. 3. Tunable linear polarization directions of YAG/Tm:YAG/YAG bulk laser as a function of polarizer angle in a plane–parallel resonator.

maximum absorbed pump power with the PER of 28 dB. As seen in Fig. 3, the peculiar case of switchable orthogonally linear polarization directions was experimentally observed. Only by carefully realigning the resonator, the linear polarization direction of output laser can be switched orthogonally, e.g., from 90° to 0°.

We evaluated the laser performance between free running and linearly polarized states in the configuration of plane–parallel resonator. Figure 4 illustrated the dependences of the output power on the absorbed pump power with $T_{\rm OC}$ of 5%.

It was found that the lasing threshold showed significant differences between free running and linearly polarized operation, e.g., 2.3 W for free running and 2.7 W for linearly polarized. The maximum output power was 2.93 W for the free running regime with the corresponding slope-efficiency of 46.7%. For each distinct linearly polarized state, the maximum output power was typically 97%–98% of the free running regime. The power optimal operation in linearly polarized state was achieved at the linear polarization angle of 170°. The maximum output power was 2.88 W, corresponding to a slope efficiency of 52.3%. The laser performance of 2 μm laser for distinct linearly polarization directions were fairly stable over the day-long operation and were easily reproducible. It's worth noting that the precise collimation for pumping beam was vital for the realization of manipulation of linearly polarized states. Linear polarization operation would not be achieved unless the typical alignment

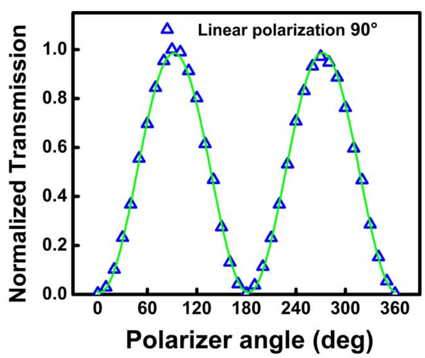

Fig. 2. Linearly polarized operation as a function of polarizer angle in a plane–parallel resonator.

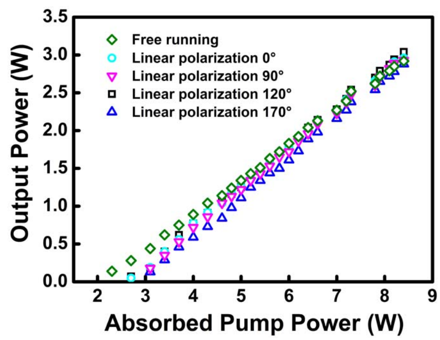

Fig. 4. Output power of free running and linearly polarized operation with plane–parallel resonator as a function of the absorbed pump power.

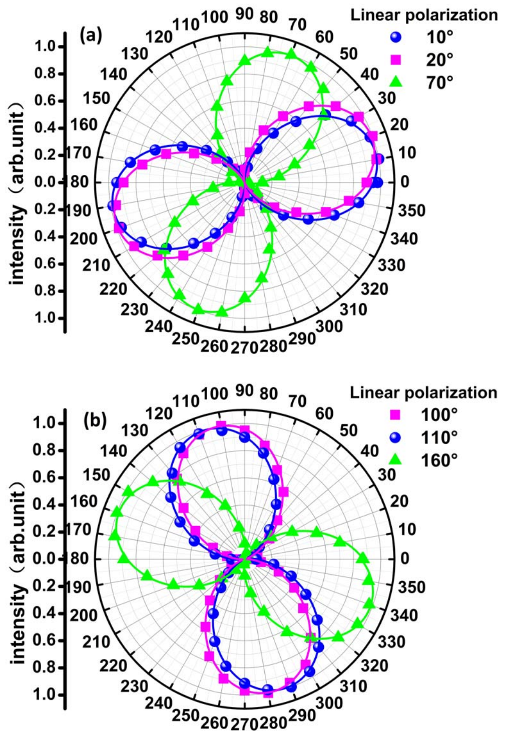

Fig. 5. Linearly polarized operation of YAG/Tm:YAG/YAG bulk laser as a function of polarizer angle in a concave–parallel resonator. (a) Three distinct linear polarization directions of 10°, 20°, and 70°. (b) Three distinct linear polarization directions of 100°, 110°, and 160°, which were orthogonal to the three linear polarization directions of (a).

tolerance angle for collimation of pumping beam is less than 0.1 mrad in our experiments.

In the following step, linearly polarized operation was further investigated in the configuration of the concave–parallel resonator with T_{OC} of 10%. An input mirror with curvature radius of 500 mm was employed. After careful realignment of the resonator, the obtained linearly polarized states with normalized transmission of output laser after passing through the polarizer as a function of polarizer angle were shown in Fig. 5.

It can be seen from Fig. 5(a) that the linear polarization directions were measured to be 10°, 20°, and 70°. We attempted to obtain the corresponding orthogonally linear polarization directions as depicted in Fig. 5(a) by carefully realigning the resonator. As shown in Fig. 5(b), three orthogonally linear polarization directions (100°, 110°, and 160°) were experimentally obtained. All these linearly polarized states of the output laser exhibited high PER with linear polarization feature (extinction ratio >26 dB). Experimental results indicated that the switchable orthogonally linear polarization directions did not depend on the transmission of output coupler and the configuration of resonator.

Figure 6 showed the laser performance of free running and linearly polarized operation in a concave–parallel resonator with T_{OC} of 10%. The slope efficiency of free running operation and linearly polarized operation at 20° and 160° were 31.2%, 31.4%, and 31.6%, respectively. The lasing threshold for free running was 2.7 W with the maximum output power of 1.75 W. Linearly polarized

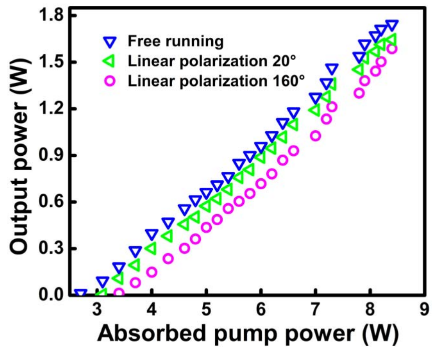

Fig. 6. Output power of free running and linear polarized operation versus the absorbed pump power in concave–parallel resonator.

operation at 20° and 160° were achieved, yielding the maximum output power of up to 1.65 W and 1.59 W and the lasing threshold of 3.1 W and 3.4 W, respectively. For a distinct linearly polarized state, the maximum output power was typically 90%–94% of the power optimal in the free running regime. It is worth noting that the threshold of free running operation was slightly lower than that of linearly polarized operation in both the plane–parallel resonator and concave–parallel resonator.

To further investigate the feature of the linearly polarized YAG/Tm:YAG/YAG crystalline laser, we aligned the resonator for obtaining the linear polarization operation under a fixed power point of absorbed pump power (e.g., 6 W). The output laser still showed a linear polarization state with high PER (typically >26 dB) in the entire range of absorbed pumped power from the above threshold to this fixed power point. However, when we continued increasing the absorbed pump power till above the fixed power point of absorbed pump power, the degree of polarization (DOP) of the output laser was found to degenerate to some extent, even to the point of being without a definite polarization characteristic. The experimental results revealed that the high DOP only achieved with the resonator alignment under the maximum absorbed pump power. If not, once the absorbed pump power reaches above the fixed power point, the polarization degeneration would be observed. It is interesting to note that more than 10 distinct linear polarization directions with high DOP can be experimentally achieved. Furthermore, the specific linear polarization direction can be switched orthogonally by realigning the resonator.

Because of the temperature sensitivity of quasi-three-level nature of the Tm:YAG laser, a figure was taken to

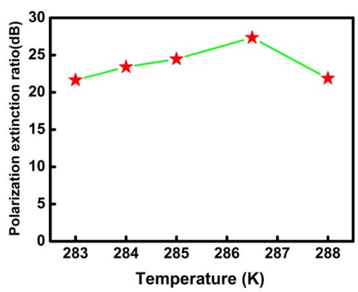

Fig. 7. Polarization extinction ratio as a function of laser crystal temperature.

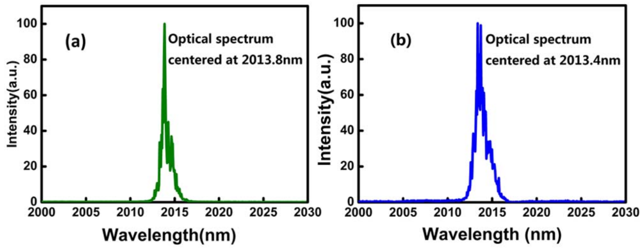

Fig. 8. (a) Spectrum of free-running regime. (b) Spectrum of linearly polarized regime.

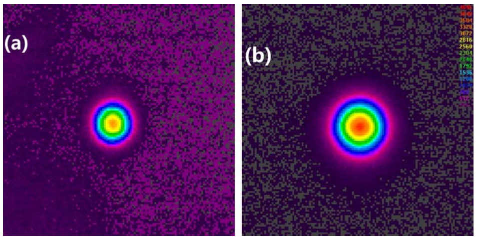

Fig. 9. (a) Beam profile of YAG/Tm:YAG/YAG bulk laser in free running operation. (b) Beam profile of YAG/Tm:YAG/YAG bulk laser in linearly polarized operation.

depict the PER as a function of the variation of laser crystal temperature controlling, as shown in Fig. 7.

We obtained the linearly polarized operation with the PER of 27.3 dB under the crystal temperature controlling of 286.5 K. The DOP of laser showed degeneration to some extent with increase or decrease of the temperature. With the temperature changing from 286.5 K to 283 K, the PER decreased from 27.3 dB to 21.6 dB. However, the output laser still exhibited high PER. According to our experimental results, the PER of a YAG/Tm:YAG/YAG bulk laser was significantly affected by varying crystal temperature control.

The spectra of free running and linearly polarized operation were measured by a Zolix Monochromator spectrograph (model Omni-λ500 with a resolution of 0.07 nm), as shown in Fig. 8. For a free-running regime, typically the laser spectrum was centered at 2013.8 nm on a 35.5 GHz-wide spectrum. As for lineraly polarized operation, the laser spectrum typically centered at 2013.4 nm on a 78.4 GHz-wide spectrum.

The beam profiles of output laser were recorded by Spiricon&Photon Laser Beam Profiler III. Seen from Figs. 9(a) and 9(b), it can be concluded that there was no significant beam quality degeneration in linearly polarized operation. The beam quality factor M^2 values were determined to be 1.2×1.3 and 1.3×1.4 for linear polarization operation and free-running operation, respectively.

In conclusion, we experimentally demonstrated the manipulation of linearly polarized states in diode-pumped YAG/Tm:YAG/YAG bulk laser operating at 2 μm simply by carefully adjusting alignment of the resonator with the help of monitoring the output power after passing through the Glan-Laser prism. Crystalline-orientation and polarized pump source independent linear polarization lasing with high DOP were observed for the first time. A 2.88 W stable linear polarization output with high PER of 28 dB had been achieved. Its maximum slope efficiency with respect to the absorbed pump power was 52.3% at 2013.4 nm. Multidistinct linear polarization directions including the switchable orthogonally directions were experimentally obtained. The linearly polarized lasing behavior exhibited several surprising features and were not completely understood. This linearly polarized lasing behavior may have been the result of an instability in the polarization state of output laser, induced by the nonlinearity and birefringence of the YAG/Tm:YAG/YAG crystal [17]. A proper mathematical model for describing the mechanism of these unexpected phenomena will be investigated in our future studies into this field.

This work had been supported by the National High-Tech R&D Program of China (Grant No. 2013AA014202) and the Knowledge Innovation Program of the Chinese Academy of Science (Grant No. KJCX2-EW-H03). We would also like to thank the financial aid of the Natural Science Foundation of Fujian province (2011J06023, 2013J05106) and Fujian High Technology Research and Development Program (Grant No. 2012H0046).

†These authors contributed equally to this work.

References

1. P. A. Budni, L. A. Pomeranz, M. L. Lemons, C. A. Miller, J. R. Mosto, and E. P. Chicklis, J. Opt. Soc. Am. B **17**, 723 (2000).
2. S. J. Augst, J. K. Ranka, T. Y. Fan, and A. Sanchez, J. Opt. Soc. Am. B **24**, 1707 (2007).
3. W. Koechner and D. K. Rice, IEEE J. Quantum Electron. **6**, 557 (1970).
4. A. R. EL-Damak, J. H. Chang, J. Sun, C. Q. Xu, and X. J. Gu, IEEE Photon. J. **5**, 1501406 (2013).
5. R. C. Stoneman and L. Esterowitz, Opt. Lett. **15**, 486 (1990).
6. R. Beach, W. J. Benett, B. L. Freitas, D. Mundinger, B. J. Comaskey, R. W. Solarz, and M. A. Emanuel, IEEE J. Quantum Electron. **28**, 966 (1992).
7. O. A. Buryy, D. Y. Sugak, S. B. Ubizskii, I. I. Izhnin, M. M. Vakiv, and I. M. Solskii, Appl. Phys. B **88**, 433 (2007).
8. A. Baum, D. Grebner, W. Paa, W. Triebel, M. Larionov, and A. Giesen, Appl. Phys. B **81**, 1091 (2005).
9. P. A. Khandokhin, Y. I. Khanin, Y. Mamaev, N. Milovskii, E. Shirokov, S. Bielawski, D. Derozier, and P. Glorieux, Quantum Electron. **28**, 502 (1998).
10. J. Dong, A. Shirakawa, and K. Ueda, Appl. Phys. Lett. **93**, 101105 (2008).
11. J. Dong, J. Ma, and Y. Y. Ren, Laser Phys. **21**, 2053 (2011).
12. J. Dong, P. Z. Deng, Y. T. Lu, Y. H. Zhang, Y. P. Liu, J. Xu, and W. Chen, Opt. Lett. **25**, 1001 (2001).
13. J. Dong, G. Z. Xu, J. Ma, M. J. Cao, Y. Cheng, K. Ueda, H. Yagi, and A. A. Kaminskii, Opt. Mater. **34**, 959 (2012).
14. A. E. C. Honea, R. J. Beach, S. B. Sutton, J. A. Speth, S. C. Mitchell, J. A. Skidmore, M. A. Emanuel, and S. A. Payne, IEEE J. Quantum Electron. **33**, 1592 (1997).
15. Y. T. Chang, Y. P. Huang, K. W. Su, and Y. F. Chen, Opt. Express **16**, 21155 (2008).
16. M. Tsunekane, N. Taguchi, and H. Inaba, Appl. Opt. **38**, 1788 (1999).
17. H. G. Winful, Opt. Lett. **11**, 33 (1986).